Public Health England

Protecting and improving the nation's health

Technical evaluation of GE Healthcare SenoClaire digital breast tomosynthesis system

NHS Breast Screening Programme Equipment Report 1404

January 2016

NHS Cancer Screening Programmes

About Public Health England

Public Health England exists to protect and improve the nation's health and wellbeing, and reduce health inequalities. It does this through world-class science, knowledge and intelligence, advocacy, partnerships and the delivery of specialist public health services. PHE is an operationally autonomous executive agency of the Department of Health.

The NHS Cancer Screening Programmes are part of Public Health England. The national office of the screening programmes is operated by PHE. It provides national management, co-ordination and quality assurance of the three cancer screening programmes for breast, cervical and bowel cancer.

Public Health England
Wellington House

133-155 Waterloo Road
London SE1 8UG
Tel: 020 7654 8000
www.gov.uk/phe
Twitter: @PHE_uk

Facebook: www.facebook.com/PublicHealthEngland

Lead authors: CJ Strudley, JM Oduko, KC Young

For queries relating to this document, contact Mary Greatorex at mary.greatorex@phe.gov.uk

The image on page 10 is courtesy of GE.

Published January 2016
PHE publications gateway number: 2015629

Acknowledgements

The authors are grateful to the staff at the Nottingham Breast Institute for making the unit available for the evaluation to be carried out.

The contribution made by P Looney of the National Coordinating Centre for the Physics of Mammography (NCCPM), who wrote the software for the data analysis, is also acknowledged.

Document Information	
Title	Technical evaluation of GE Healthcare SenoClaire digital breast tomosynthesis system
Policy/document type	Equipment Report 1404
Electronic publication date	January 2016
Version	1
Superseded publications	None
Review date	None
Author/s	CJ Strudley , JM Oduko, KC Young
Owner	NHS Breast Screening Programme
Document objective (clinical/healthcare/social questions covered)	To provide an evaluation of this equipment's suitability for use within the NHSBSP
Population affected	Women eligible for routine and higher-risk breast screening
Target audience	Physicists, radiographers, radiologists
Date archived	Current document

Contents

Executive summary

The purpose of this evaluation was to measure the technical performance of the GE Healthcare SenoClaire digital breast tomosynthesis system. The technical performance was tested in both 2D and tomosynthesis modes. Upgrading the GE Healthcare Essential for tomosynthesis required the installation of a removable Motorised Tomosynthesis Device (MTD), which may be used for both tomosynthesis and 2D imaging. Using the MTD in 2D mode gave a similar performance to that when using the standard 2D Bucky and met current NHSBSP standards for digital mammography. No performance standards have yet been set for digital breast tomosynthesis systems and it is not possible to compare performance of different systems using the results in this report.

The mean glandular dose to the standard breast was measured in tomosynthesis mode and found to be close to the dose measured in 2D mode. The results in this report may be useful for comparison with quality assurance measurements on other SenoClaire systems.

1. Introduction

1.1 Testing procedures and performance standards for digital mammography

Testing procedures and performance standards for conventional 2D mammography are well established and documented[1-3] but at the time of the evaluation there were no nationally agreed procedures and standards for digital breast tomosynthesis (DBT) systems. The tests of tomosynthesis performance employed for this evaluation were the same as those used in the evaluations of tomosynthesis systems from Hologic[4] and Siemens[5]. All these tests were based on those used for the TOMMY trial.[6]

The technical performance of the 2D GE Healthcare Senographe Essential system has previously been assessed and reported.[7, 8] For this evaluation, the SenoClaire tomosynthesis system was installed as an extension to a Senographe Essential. This provided an additional mode of 2D operation, as well as the tomosynthesis facility. The technical performance of the equipment operating in tomosynthesis mode and in both of the available 2D modes was assessed.

The results presented in this report may be indicative of clinical performance. However, research to assess the clinical effectiveness of tomosynthesis is ongoing and further work is required to establish corresponding measures of technical performance. Until this is done, it is not possible to compare different systems.

1.2 Objectives

This evaluation of the GE Healthcare SenoClaire tomosynthesis system had two objectives. The first was to ensure that the 2D performance of the tomosynthesis system met the main standards in the NHSBSP and European protocols. The second was to measure the performance of the system in tomosynthesis mode, for comparison with quality assurance measurements on other SenoClaire systems.

2. Methods

2.1 System tested

The system tested was an existing GE Healthcare Senographe Essential that had been upgraded with the SenoClaire tomosynthesis system to perform digital breast tomosynthesis as well as 2D digital mammography. The upgrade includes a removable Motorised Tomosynthesis Device (MTD), which the operator attaches in place of the standard 2D Bucky. 2D imaging is performed either using the standard 2D Bucky or using the MTD in 2D mode. The MTD may be used for both 2D and tomosynthesis imaging, if it is left permanently in place. The operator selects the tomosynthesis option by pressing the “3D” button on the MTD. The MTD has a special anti-scatter grid used for both 2D and tomosynthesis imaging. A specific set of compression paddles (including a sliding 18cm x 24cm paddle) is provided for use with the MTD, for both tomosynthesis and 2D imaging.

Three automatic exposure control (AEC) modes are available for 2D imaging: *Standard*, *Contrast* and *Dose*. For tomosynthesis imaging, only one mode is available. Standard mode was used for all exposures under AEC in this evaluation. For all modes, a preliminary exposure with a tube load of 4mAs is used to determine beam quality and tube load.

To acquire both 2D and tomosynthesis exposures in the same compression, the automatic decompression of the breast must be disabled. After the first exposure, the

operator has to go to the X-ray set and press the “3D” button to change mode, before making the second exposure. After both exposures, the operator may initiate decompression from the console.

During a tomosynthesis acquisition, the X-ray tube rotates about a centre of rotation located 40mm above the detector and approximately 18mm above the breast support table. The tube always moves away from the woman’s head during tube rotation, from a starting position at an angle of ±15.6°, depending on the positioning of the woman. The preliminary exposure is made at ±12.5° (or at ±15.6° or ±9.4° if an offset is used with a small field of view). This uses a tube voltage and target filter combination selected according to the compressed breast thickness. The image from the preliminary exposure is used to adjust the tube voltage and target filter selection, if necessary, and to calculate the tube load for the tomosynthesis projection images. The first tomosynthesis projection is acquired at the same position as the preliminary exposure and a further eight projection images are acquired at 3.1° intervals. The tube is stationary for each exposure; this is known as “step-and-shoot”. The total acquisition covers a range of 25°. Collimation is dynamic and adjusts during the tomosynthesis exposure to restrict the radiation field to the detector, which remains stationary.

The raw projections are sent from the acquisition workstation to a reconstruction workstation where reconstruction is performed using an iterative algorithm. The reconstructed tomosynthesis images are unaffected by operator selection of image processing at the acquisition workstation. Two reconstructed volumes are produced. The first volume consists of reconstructed focal planes spaced at intervals of either 0.5mm or 1mm, as configured at system installation. The second volume is created from the first and contains slabs representing 10mm thicknesses of tissue, which are spaced at 5mm intervals so that adjacent slabs overlap. The reconstructed volumes are then sent to the Image Diagnost International (IDI) viewing workstation, from where they may be downloaded for analysis. Only 2D images can be downloaded directly from the acquisition workstation. At the IDI workstation, a synthetic 2D view may be created from the tomosynthesis projections, but this is not available for download and therefore was not assessed in this evaluation.

Both the volumes containing focal planes and the volumes containing slabs were assessed in some of the tomosynthesis tests. The system tested was configured to reconstruct focal planes at 0.5mm intervals. Details of the system are given in Table 1.

QC images can be downloaded from the IDI viewing workstation via a USB port. The tomosynthesis images are in the DICOM[9] BTO format. Typical image file sizes are shown in Table 2.

Table 1. System description

Manufacturer	GE
Model	SenoClaire
System serial number	104520220154203
Target material	Molybdenum Rhodium
Added filtration	30µm molybdenum for molybdenum target 25µm rhodium for either molybdenum or rhodium target
Detector type	Caesium iodide with amorphous silicon flat panel
Detector serial number	PLC0020_01
Pixel size	100µm in 2D and projection images and in reconstructed focal planes and slabs
Detector area	239mm x 306mm; 191mm x 229mm
Pixel array	2394 x 3062; 1914 x 2294
Pixel value offset	0
AEC Modes	Standard, Contrast, Dose for 2D; Standard for tomosynthesis
AEC pre-exposure pulse	4mAs
Tomosynthesis projections	9 equal dose projections at 3.1° intervals giving a total angular range of 25°
Reconstructed focal planes	Vertical intervals: 0.5mm or 1mm as configured Number of planes: 2 x (CBT in mm) + 10 for 0.5mm spacing
Reconstructed slabs	10mm thick, at 5mm vertical intervals
Software version	ADS Application Package version ADS_56.10

Table 2. 2D and tomosynthesis image file sizes for 60mm compressed breast thickness

	Small format (191mm x 229mm)	Large format (239mm x 306mm)
2D	8MB	14MB
Tomosynthesis focal planes (0.5mm spacing)	1.1GB	1.8GB
Tomosynthesis slabs	110MB	190MB

The tomosynthesis system is shown in Figure 1.

Figure 1. The GE Healthcare SenoClaire digital breast tomosynthesis system

2.2 Dose and contrast-to-noise ratio under AEC

Dose and contrast-to-noise ratio (CNR) were measured using the AEC to expose a range of thicknesses of Perspex (polymethylmethacrylate or PMMA). The mean glandular dose (MGD) to the standard breast was calculated for the equivalent breast thicknesses. For CNR measurements, a square of aluminium 0.2mm thick was included in the phantom.

2.2.1 Dose measurement

To calculate the MGD to the standard breast, measurements were made of half value layer (HVL) and tube output, over the clinically relevant range of kV and target /filter combinations. The output measurements were made on the midline at the standard

position of 40mm from the chest wall edge (CWE) of the breast support platform. As the system uses the same range of tube voltages and target filter combinations for both tomosynthesis and 2D imaging, the output measurements were made in 2D mode only. The paddle was in the beam, raised well above the ion chamber.

In both 2D and tomosynthesis modes, exposures of a range of thicknesses of PMMA were made under AEC (Standard mode). For each thickness, spacers were used to create an air gap between the top of the PMMA and the paddle so that the correct equivalent breast thickness was displayed by the compressed breast thickness indicator. The spacers were positioned across the back edge of the phantom to avoid interference with the rest of the tomosynthesis image.

Doses in 2D mode were calculated as described in the UK protocol[1]. Doses in tomosynthesis mode were calculated using the method described by Dance et al.[10]. This is an extension of the established 2D method, using the equation:

$$D = KgcsT \quad (1)$$

where K is the incident air kerma at the top surface of the breast, and g, c and s are conversion factors. The additional factor, T, is derived by summing weighted correction factors for each of the tomosynthesis projections. Values of T are tabulated[10] for the SenoClaire system for different compressed breast thicknesses.

The Dance method of calculating MGD uses a measured dose at the surface of the breast with the paddle in contact, but the method described in the UK protocol differs in that dose is measured with the paddle raised well above the ion chamber. To allow comparisons to be made with systems for which dose measurements have been made according to the UK protocol, MGD results in this report are calculated with the paddle raised. Measurements with the paddle in contact with the ion chamber have been found to give results a few percent higher[4].

2.2.2 CNR

For CNR measurements a 10mm x 10mm square of 0.2mm thick aluminium foil was included in the phantom, positioned 10mm above the table on the midline, 60mm from the CWE.

CNR in 2D images was assessed using 5mm x 5mm regions of interest (ROIs) positioned in the centre of the aluminium square and at two background positions on the chest wall and nipple sides of the square.

CNR was measured in tomosynthesis focal planes, and in slabs, using 5mm x 5mm ROIs placed at the same positions as used for 2D CNR, as shown in Figure 2. The CNR was measured in the focal plane or slab in which the aluminium square was brought into best focus. CNR was also measured in the unprocessed tomosynthesis projections using a 5mm x 5mm ROI.

Variation of CNR with dose in tomosynthesis mode was assessed both in the projections and in the reconstructed images (planes and slabs) for an equivalent breast thickness of 53mm (that is, using a 45mm thickness of PMMA).

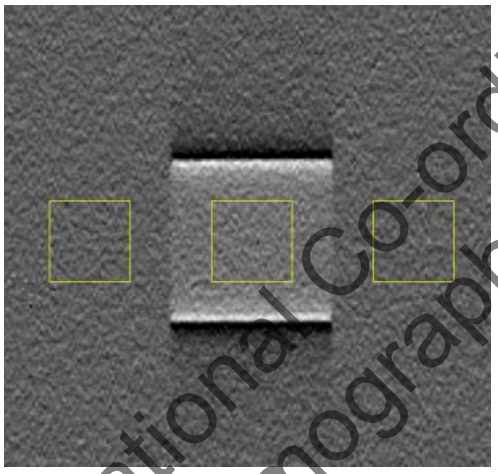

Figure 2. Position of 5mm x 5mm ROIs for measurement of CNR in tomosynthesis (CWE on the right)

2.3 Image quality measurements

Image quality was assessed in 2D mode using a CDMAM phantom. In the absence of a suitable test object for assessing tomosynthesis imaging performance, images of the CDMAM were also acquired in tomosynthesis mode. The CDMAM phantom (Version 3.4, serial number 1022, UMC St. Radboud, Nijmegen University, Netherlands) was positioned between two blocks of PMMA, each 20mm thick. The exposure factors used were the same as those selected by the AEC for an equivalent breast thickness of 60mm. One set of sixteen images was acquired in 2D mode at the AEC selected dose, using the standard 2D Bucky. With the 2D Bucky replaced by the MTD, sets of sixteen CDMAM images in both 2D mode and tomosynthesis mode were acquired at the AEC selected dose. A further two sets were acquired at half and double this dose. (Only seven images were downloaded at double the dose).

In tomosynthesis mode, image quality was assessed in the focal plane or slab of best focus, at the height of the CDMAM above the table. This plane or slab was extracted using software developed in-house. Both sets of 2D images and the sets of

tomosynthesis images were read and analysed using two software tools, CDCOM version 1.6, (available from www.euref.org, accessed 04 July 2013) and CDMAM Analysis version 1.4 (available from www.nccpm.org, accessed July 2013). The process was repeated using the planes immediately above and below the expected plane of best focus. This ensured that the CDMAM result quoted was for the focal plane corresponding to the best image quality.

2D image quality assessed using the CDMAM is for an equivalent breast thickness of 60mm. This can be related to the image quality at other thicknesses by comparing the CNRs measured for a range of thicknesses. The European protocol[2] gives the relationship between threshold contrast and CNR measurements, enabling calculation of a target CNR value for a particular level of image quality. This can be compared to CNR measurements made at other breast thicknesses. Contrast for a particular gold thickness is calculated using Equation 2, and target CNR is calculated using Equation 3.

$$\text{Contrast} = 1e^{-\mu t} \quad (2)$$

where μ is the effective attenuation coefficient for gold, and t is the gold thickness.

$$\text{CNR}_{\text{target}} = \frac{\text{CNR}_{\text{measured}} \text{ x } \text{TC}_{\text{measured}}}{\text{TC}_{\text{target}}} \quad (3)$$

where $\text{CNR}_{\text{measured}}$ is the CNR for a 60mm equivalent breast, $\text{TC}_{\text{measured}}$ is the threshold contrast calculated using the threshold gold thickness for a 0.1mm diameter detail (measured using the CDMAM at the same dose as used for $\text{CNR}_{\text{measured}}$), and $\text{TC}_{\text{target}}$ is the calculated threshold contrast corresponding to the threshold gold thickness required to meet either the minimum acceptable or achievable level of image quality. The 0.1mm detail threshold gold thickness is used here because it is generally regarded as the most critical size for which performance standards are set.

The effective attenuation coefficient for gold used in Equation 2 depends on the beam quality used for the exposure, and was selected from the values shown in Table 3. These values were calculated[11] for a caesium iodide detector, with 3mm PMMA representing the compression paddle. Spectra from Boone et al.[12] and attenuation coefficients for materials in the test objects (aluminium, gold, PMMA) from Berger et al.[13] were used in these calculations.

The European protocol also defines a limiting value for CNR, which is a percentage of the threshold contrast for minimum acceptable image quality for each thickness. The target CNR values for minimum acceptable and achievable levels of image quality and the European limiting values for CNR were calculated. These are compared with the CNR results in Section 3.2.

The calculated target CNRs can be used to estimate the dose required to meet those standards, using the relationship given in Equation 4. This assumes that the dominant noise component is quantum noise.

$$\mathrm{Dose}_{\mathrm{target}} = \mathrm{Dose}_{\mathrm{measured}} \left(\frac{\mathrm{CNR}_{\mathrm{target}}}{\mathrm{CNR}_{\mathrm{measured}}}\right)^2 \quad (4)$$

where $\mathrm{Dose}_{\mathrm{measured}}$ is the MGD corresponding to $\mathrm{CNR}_{\mathrm{measured}}$.

Table 3. Effective attenuation coefficients for gold contrast details in the CDMAM

kV	Target	Filter	Effective attenuation coefficient
25	Mo	Mo	0.179
28	Mo	Mo	0.157
31	Mo	Mo	0.135
25	Mo	Rh	0.153
28	Mo	Rh	0.143
31	Mo	Rh	0.130
25	Rh	Rh	0.144
28	Rh	Rh	0.132
31	Rh	Rh	0.121

2.4 Geometric distortion and reconstruction artefacts

The relationship between reconstructed tomosynthesis focal planes and the physical geometry of the volume that they represent was assessed. This was done by imaging a geometric test phantom consisting of a rectangular array of 1mm diameter aluminium balls, 50mm apart, in the middle of a 5mm thick sheet of PMMA. The phantom was placed at various heights (7.5, 32.5, and 52.5mm) above the breast support table within a 60mm stack of plain sheets of PMMA. The paddle was then raised to 120mm above the table, with the phantom attached to its underside, and an additional tomosynthesis image was acquired. The nominal height of the balls in this case was 117.5mm.

Reconstructed tomosynthesis planes were analysed to find the height of the focal plane in which each ball was best in focus, the position of the centre of the ball within that plane, and the number of adjacent planes in which the ball was also seen. The variation in appearance of the ball between focal planes was quantified.

This analysis was automated through the use of an ImageJ (available at rsb.info.nih.gov/ij) plug-in, developed in-house by NCCPM for this purpose.

2.4.1 Height of best focus

For each ball, the height of the focal plane in which it was best in focus was identified. Results were compared for all balls within each image, to judge whether there was any tilt of the test phantom relative to the reconstructed planes, or any vertical distortion of the focal planes within the image.

2.4.2 Positional accuracy within focal plane

The x and y co-ordinates within the image were found for each ball. (x and y are perpendicular and parallel to the CWE, respectively). The mean distances between adjacent balls were calculated, using the pixel spacing quoted in the DICOM image header. This was compared to the physical separation of balls within the phantom, to assess the scaling accuracy in the x and y directions. The maximum deviations from the mean x and y separations were calculated, to indicate whether there was any discernible distortion of the image within the focal plane.

2.4.3 Appearance of the ball in adjacent focal planes

Changes to the appearance of a ball in different focal planes were assessed visually.

To quantify the extent of reconstruction artefacts in adjacent focal planes, the reconstructed image was treated as though it were a true three dimensional volume. A software tool was used to find the x, y, and z dimensions of a volume around each ball which would enclose all pixels with values exceeding 50% of the maximum pixel value. The method used was to create a composite x-y image using the maximum pixel values from all focal planes. A composite x line was then created using the maximum pixel from each column of the x-y composite plane. The full width at half maximum (FWHM) in the x direction was found by fitting a polynomial spline. This was repeated in the orthogonal direction to produce the y-FWHM, and again using vertical re-sliced planes to find the z-FWHM. All pixel values were background subtracted, using the mean pixel value from around the ball in the plane of best focus. The composite z-FWHM thus calculated was used as a measure of the inter-plane resolution, or z-resolution. Its value would be different if a ball of different size were used.

The FWHM in the x and y directions of the image of the ball were also measured in the plane of best focus, in order to compare against the composite x- and y-FWHM measurements, so that any apparent shift or spread in the appearance of the ball through a series of adjacent focal planes could be quantified.

2.5 Alignment

Alignment measurements were carried out for reconstructed tomosynthesis images.

The alignment of the X-ray beam to the focal plane at the surface of the breast support table was assessed. Self-developing film and graduated markers were positioned on each edge of the X-ray beam as indicated by the light field. The alignment at the lateral edges was only measured at this height because at other heights the movement of the tube during the scan would cause the lateral edges of the X-ray beam to move between projections.

The alignment of the imaged volume to the compressed volume was assessed at the top and bottom of the volume. Missed tissue at the CWE was not assessed for this evaluation. Small high contrast markers were placed on the breast support table and on the underside of the compression paddle to assess vertical alignment. The image planes were then inspected to check whether all markers were brought into focus within the reconstructed tomosynthesis volume. To make measurements with the paddle at both extremes of its flexion, images were first acquired with no compression applied and then repeated with the CWE of the paddle supported and 9kg compression applied.

2.6 Image uniformity and repeatability

The reproducibility of the reconstructed tomosynthesis images was tested by acquiring a series of 16 images of a 45mm thick block of PMMA under AEC. A 10mm x 10mm ROI was positioned 60mm from the CWE in the plane corresponding to a height of 22.5mm above the breast support table. To calculate the signal-to-noise ratio (SNR) for each image, the mean and standard deviation of the pixel values were found in this ROI. The exposure factors selected by the AEC were obtained from the DICOM header for each image. These images and others acquired during the evaluation were also visually inspected for artefacts.

2.7 Detector response

Detector response was measured in both 2D and tomosynthesis modes, using the MTD. The anti-scatter grid remained in place as it is not possible to use the MTD without the grid. An aluminium filter, 2mm thick, was placed in the beam and attached to the tube port. A typical beam quality, 29kV Rh / Rh, was selected and images were acquired using a range of tube load settings in both tomosynthesis and 2D modes. The mean pixel value was measured in a 10mm x 10mm ROI positioned on the midline 50mm from the CWE of each raw unprocessed 2D image or projection. These were plotted against tube load. For tomosynthesis images, the tube load used was the mAs per projection.

3. Results

3.1 Output and HVL

The tube output and HVL are shown in Table 4.

Table 4. Tube output measurement and HVL

kV	Target	Filter	Tube output (µGy/mAs at 1m)	HVL (mm Al)
26	Mo	Mo	27.6	0.34
26	Mo	Rh	22.4	0.40
28	Rh	Rh	26.3	0.42
31	Rh	Rh	35.9	0.46

3.2 Dose and CNR

The doses measured for 2D imaging, with both the standard Bucky and the MTD, and for tomosynthesis, are shown in Tables 5, 6 and 8, and are presented graphically in Figure 3.

The CNR measurements for 2D images are shown in Tables 5 and 6. CNR measurements for focal planes and slabs in the reconstructed tomosynthesis images and for the central (zero degree) projection images are shown in Table 8. The CNR results for 2D and tomosynthesis are also presented graphically in Figures 4 and 5. Figure 4 includes the target levels of CNR required for the NHSBSP minimum acceptable and achievable levels of 2D image quality (9.7 and 14.4 respectively for the 2D Bucky, 10.1 and 14.9 for the MTD), as calculated using the CDMAM results (Section 3.3). Results are presented for equivalent breast thicknesses up to 117mm. The European limiting values of CNR are also shown; these are only set for thicknesses up to 90mm.

Table 7 shows the estimated mean glandular dose, to a 60mm thick equivalent breast, required to meet the minimum acceptable and achievable levels of image quality for 2D imaging. For comparison, the values reported in a previous evaluation of the GE Healthcare Essential[7] are also shown.

Table 5. Dose and CNR using the 2D Bucky in AEC standard mode

PMMA thickness (mm)	Equivalent breast thickness (mm)	kV	Target / filter	mAs*	MGD (mGy)	NHSBSP 2D dose limit (mGy)	CNR
20	21	26	Mo / Mo	26.5	0.70	1.0	27.3
30	32	26	Mo / Rh	43.6	0.82	1.5	20.7
40	45	27	Mo / Rh	60.2	1.06	2.0	17.6
45	53	29	Rh / Rh	56.0	1.13	2.5	16.1
50	60	29	Rh / Rh	64.2	1.21	3.0	14.4
60	75	30	Rh / Rh	91.7	1.77	4.5	13.1
70	90	31	Rh / Rh	113.9	2.14	6.5	12.4
80	108	31	Rh / Rh	203.0	3.27	-	10.6
85	117	31	Rh / Rh	277.6	4.52	-	10.9

*The mAs recorded here is the total mAs including the preliminary exposure (tube load 4mAs), which is not included in the image

Table 6. Dose and CNR for 2D images using the MTD in AEC standard mode

PMMA thickness (mm)	Equivalent breast thickness (mm)	kV	Target / filter	mAs*	MGD (mGy)	NHSBSP 2D dose limit (mGy)	CNR
20	21	26	Mo / Mo	31.9	0.84	1.0	28.1
30	32	26	Mo / Rh	47.4	0.89	1.5	20.8
40	45	29	Rh / Rh	48.3	1.07	2.0	17.7
45	53	29	Rh / Rh	64.0	1.29	2.5	16.8
50	60	29	Rh / Rh	74.2	1.40	3.0	15.3
60	75	30	Rh / Rh	99.7	1.92	4.5	13.8
70	90	31	Rh / Rh	147.6	2.78	6.5	12.7
80	108	31	Rh / Rh	244.1	3.93	-	11.7
85	117	31	Rh / Rh	324.0	5.27	-	11.5

*The mAs recorded here is the total mAs including the preliminary exposure (tube load 4mAs), which is not included in the image

Table 7. Estimated doses to a 60mm equivalent breast to achieve the CNR values corresponding to the minimum acceptable and achievable levels of image quality

	MGD with 2D Bucky (mGy)	MGD with MTD in 2D mode (mGy)	MGD from previous GE Essential evaluation (mGy)
Minimum acceptable level	0.52 ± 0.10	0.58 ± 0.12	0.49 ± 0.10
Achievable level	1.13 ± 0.23	1.26 ± 0.25	1.13 ± 0.23

Table 8. Dose and CNR for tomosynthesis images acquired under AEC

PMMA thickness (mm)	Equivalent breast thickness (mm)	kV	Target / filter	mAs*	MGD (mGy)	CNR in focal planes	CNR in slabs	CNR in central projection
20	21	26	Mo / Mo	35	0.91	6.2	5.5	9.4
30	32	29	Rh / Rh	32	0.86	4.9	4.5	6.9
40	45	29	Rh / Rh	50	1.09	5.2	4.7	5.7
45	53	29	Rh / Rh	55	1.09	5.1	4.7	4.9
50	60	29	Rh / Rh	73	1.35	5.2	4.8	4.9
60	75	31	Rh / Rh	84	1.79	5.3	4.8	4.2
70	90	31	Rh / Rh	142	2.61	5.7	5.1	3.9
80	108	31	Rh / Rh	240	3.77	6.0	5.3	3.6
85	117	31	Rh / Rh	296	4.69	5.9	5.3	3.5

*The mAs recorded here is the total mAs including the preliminary exposure (tube load 4mAs), which is not included in the reconstructed tomosynthesis image

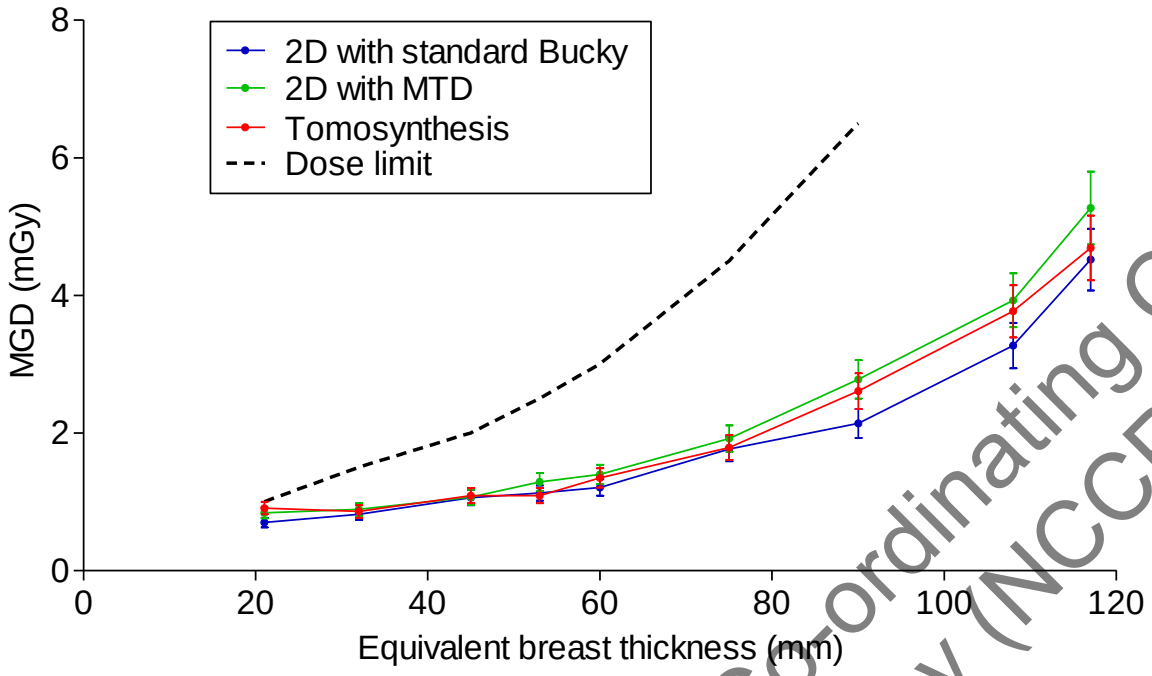

Figure 3. MGD for 2D and tomosynthesis exposures under AEC. (Error bars indicate 95% confidence limits.)

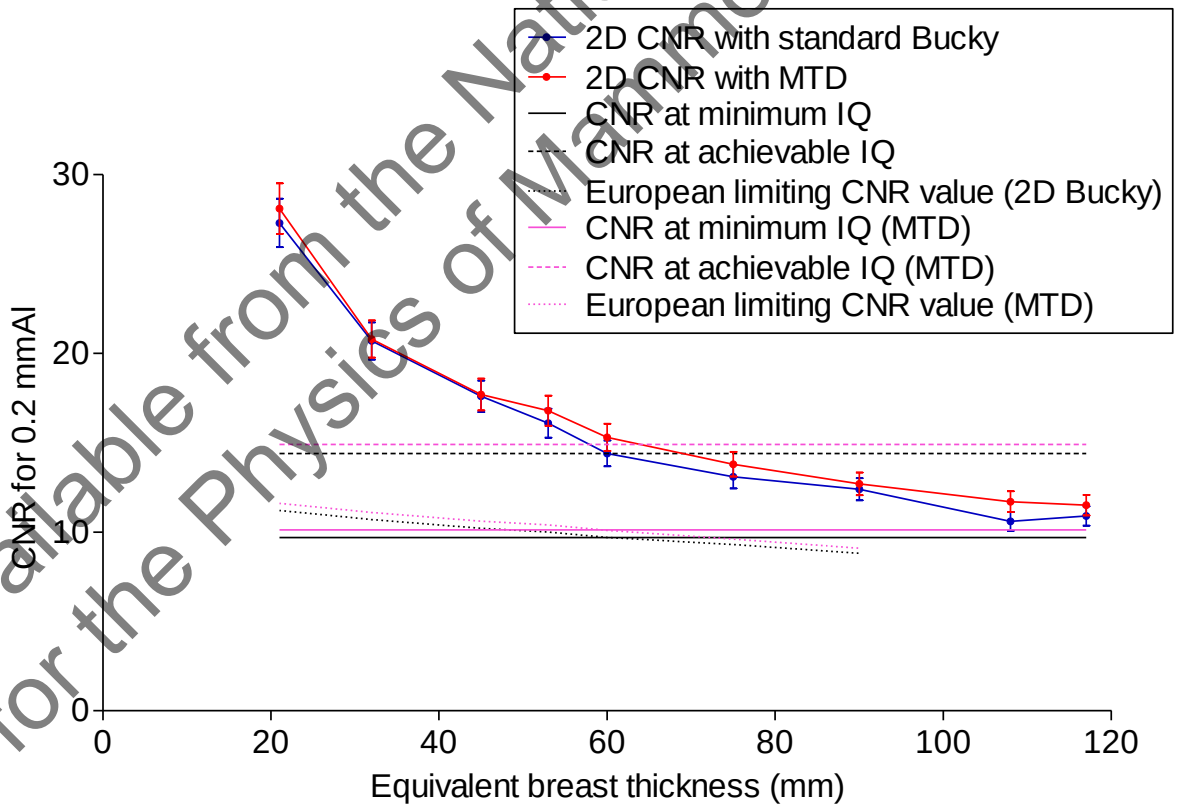

Figure 4. CNR for 2D images obtained under AEC, compared with limiting values from the European protocol. (Error bars indicate 95% confidence limits.)

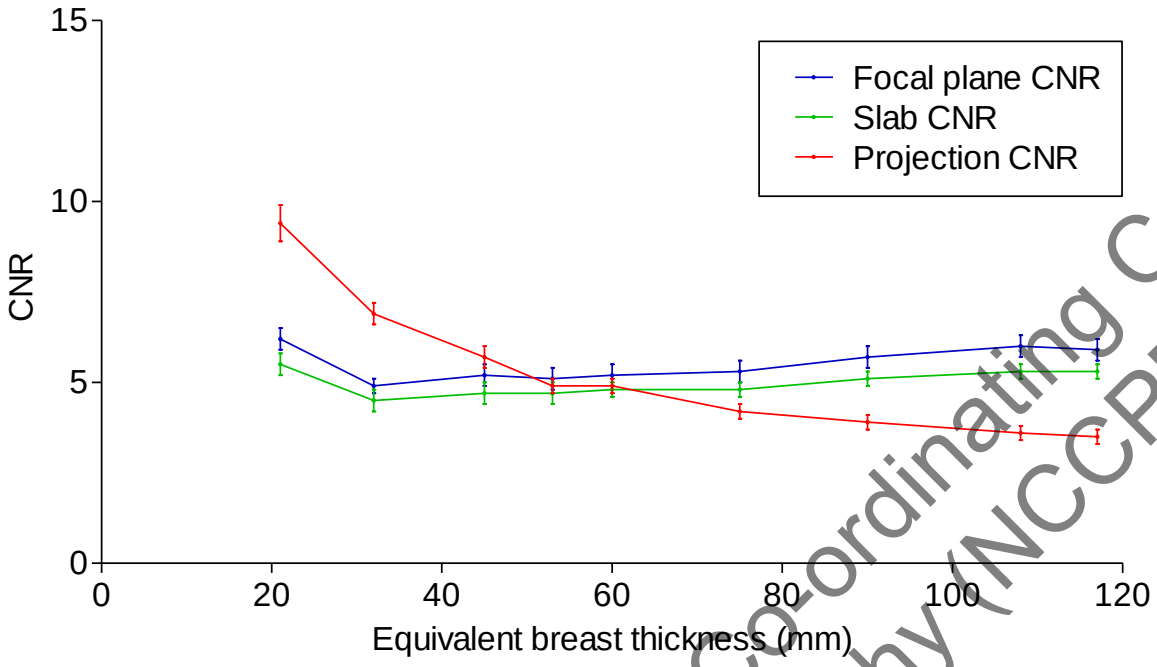

Figure 5. CNR for tomosynthesis images obtained under AEC. (Error bars indicate 95% confidence limits.)

The variation of CNR with dose in tomosynthesis mode is shown in Table 9 and Figure 6. The CNR was measured in the reconstructed focal plane and slab where the aluminium square was best in focus and in the central projection image. A power fit was applied to the relationship between CNR and dose for reconstructed focal planes, slabs and projections, shown in Figure 6.

Table 9 Variation of CNR with dose in tomosynthesis mode

PMMA (mm)	Equivalent breast thickness (mm)	kV	Target / filter	mAs	MGD (mGy)	CNR in reconstructed DBT image	CNR in slab	CNR in central projection
40	45	29	Rh / Rh	36	0.78	4.1	3.6	3.9
40	45	29	Rh / Rh	63	1.37	5.0	4.5	5.5
40	45	29	Rh / Rh	100	2.17	6.0	5.3	7.4
40	45	29	Rh / Rh	160	3.48	7.2	6.4	9.4
40	45	29	Rh / Rh	250	5.43	8.2	7.4	11.6

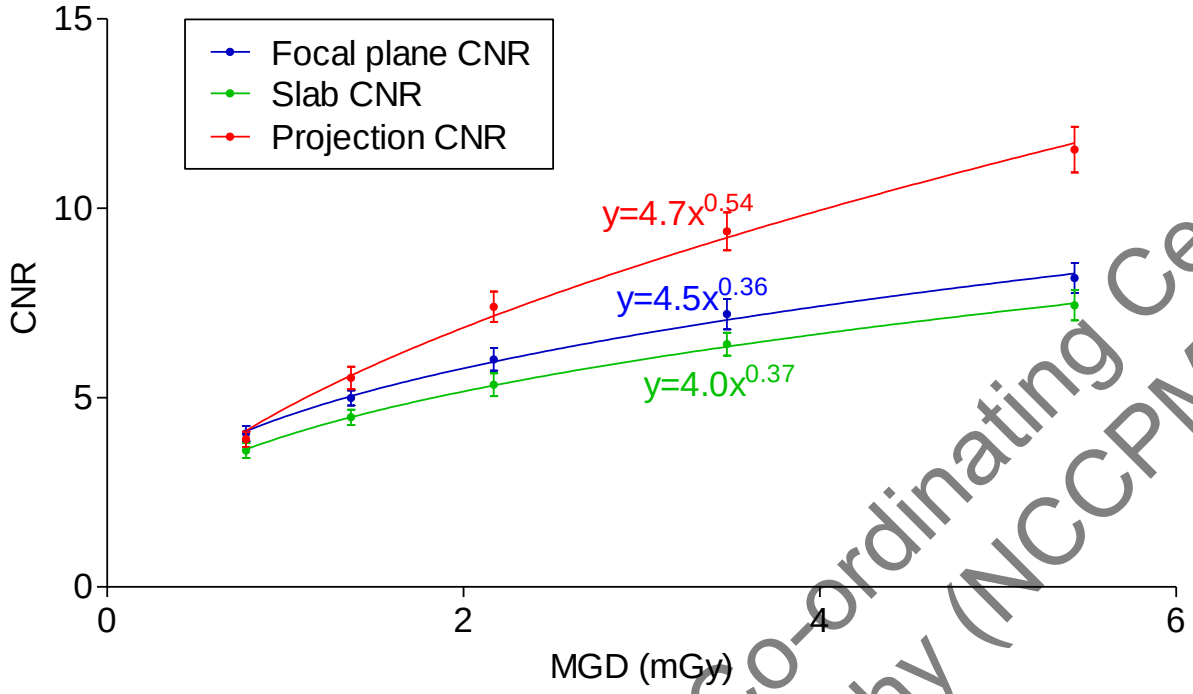

Figure 6. CNR for a 53mm thick equivalent breast at a range of doses in tomosynthesis mode. (Error bars indicate 95% confidence limits.)

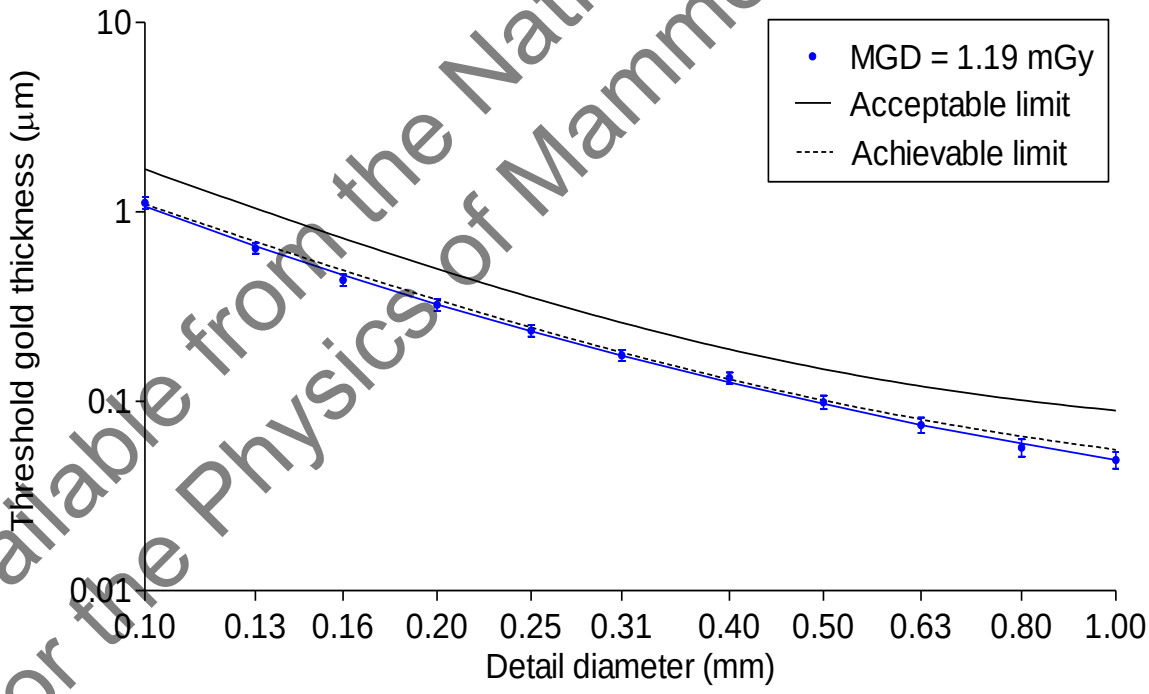

Figure 7. Threshold gold thicknesses for 2D images acquired using the 2D Bucky at the dose selected under AEC at 29kV Rh / Rh. (Error bars indicate 95% confidence limits.)

3.3 Image quality measurements

The threshold gold thickness results in this section are predicted human results as calculated for 2D mammography.

The contrast detail curve for 2D images using the 2D Bucky is shown in Figure 7. Figure 8 shows the curves for 2D images using the MTD, at the AEC selected dose and at half and twice this dose.

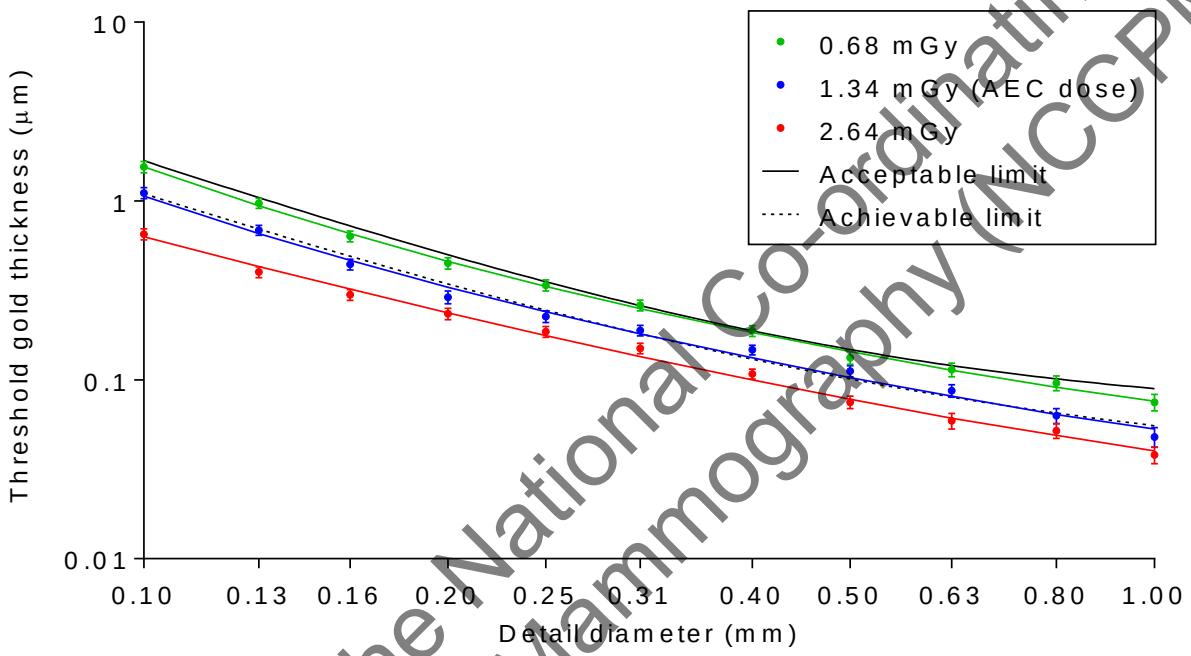

Figure 8. Threshold gold thicknesses for 2D images acquired using the MTD at three doses at 29kV Rh / Rh. (Error bars indicate 95% confidence limits.)

The 2D image quality results shown in Figures 7 and 8 are summarised in Table 10.

Table 10. Fit to predicted threshold gold thickness for CDMAM images, acquired using both the 2D Bucky and the MTD (2D mode)

	Threshold gold thickness (µm)					
Detail diameter (mm)	2D Bucky AEC dose 1.19mGy	2D MTD AEC dose 1.34mGy	2D MTD Half AEC dose 0.68mGy	2D MTD Double AEC dose 2.64mGy	Minimum standard for 2D	Achievable standard for 2D
0.1	1.069	1.064	1.554	0.632	1.680	1.100
0.25	0.234	0.240	0.333	0.177	0.352	0.244
0.5	0.097	0.103	0.144	0.078	0.150	0.103
1.0	0.049	0.053	0.076	0.040	0.091	0.056

Figure 9 shows the CDMAM curves for five adjacent focal planes from the tomosynthesis images acquired at the AEC selected dose. The lowest threshold gold thicknesses were obtained for focal plane 46.

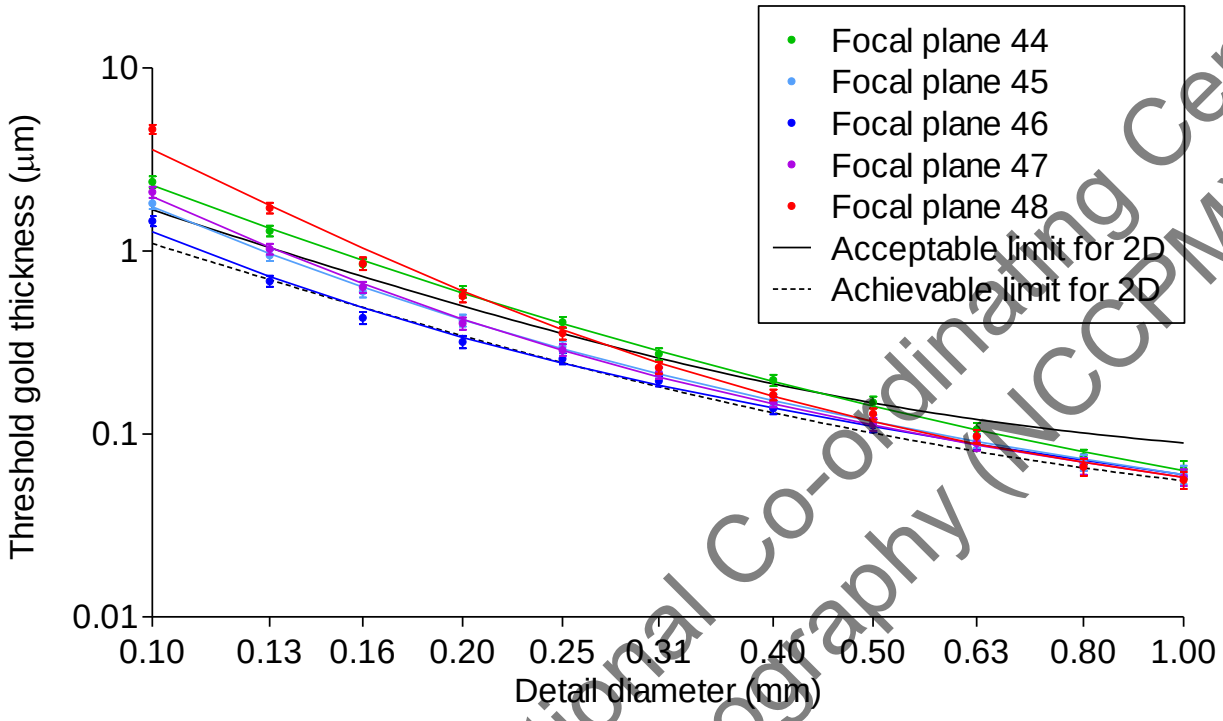

Figure 9. Threshold gold thicknesses for reconstructed focal planes taken from CDMAM images acquired in tomosynthesis mode at the AEC selected dose at 29kV Rh / Rh. (Error bars indicate 95% confidence limits.)

Figure 10 shows the CDMAM curves for focal plane 46 from the images acquired at the AEC selected dose and at half and double this dose.

Figure 11 shows the CDMAM results from the reconstructed volumes containing 10mm slabs. These curves are for slab 5, the only slab in which the gold details were seen in focus.

The image quality results shown in Figures 10 and 11 are summarised in Table 11.

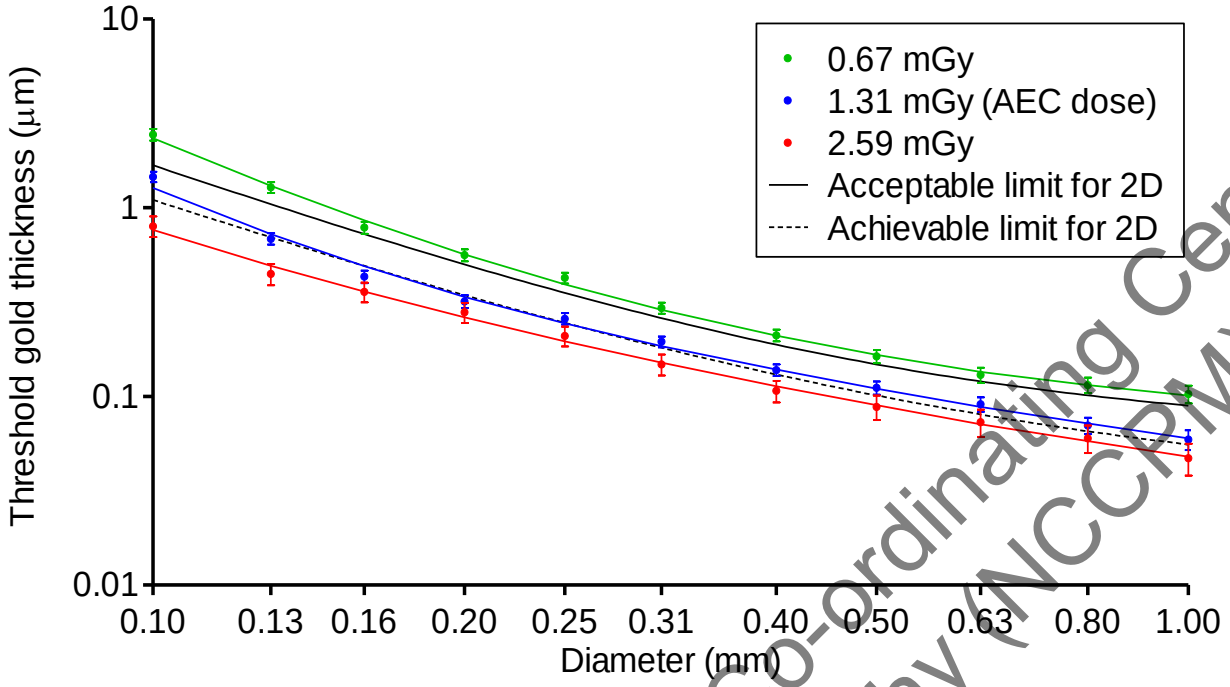

Figure 10. Threshold gold thicknesses for reconstructed focal plane 46 taken from tomosynthesis CDMAM images acquired in tomosynthesis mode at three doses at 29kV Rh / Rh. (Error bars indicate 95% confidence limits.)

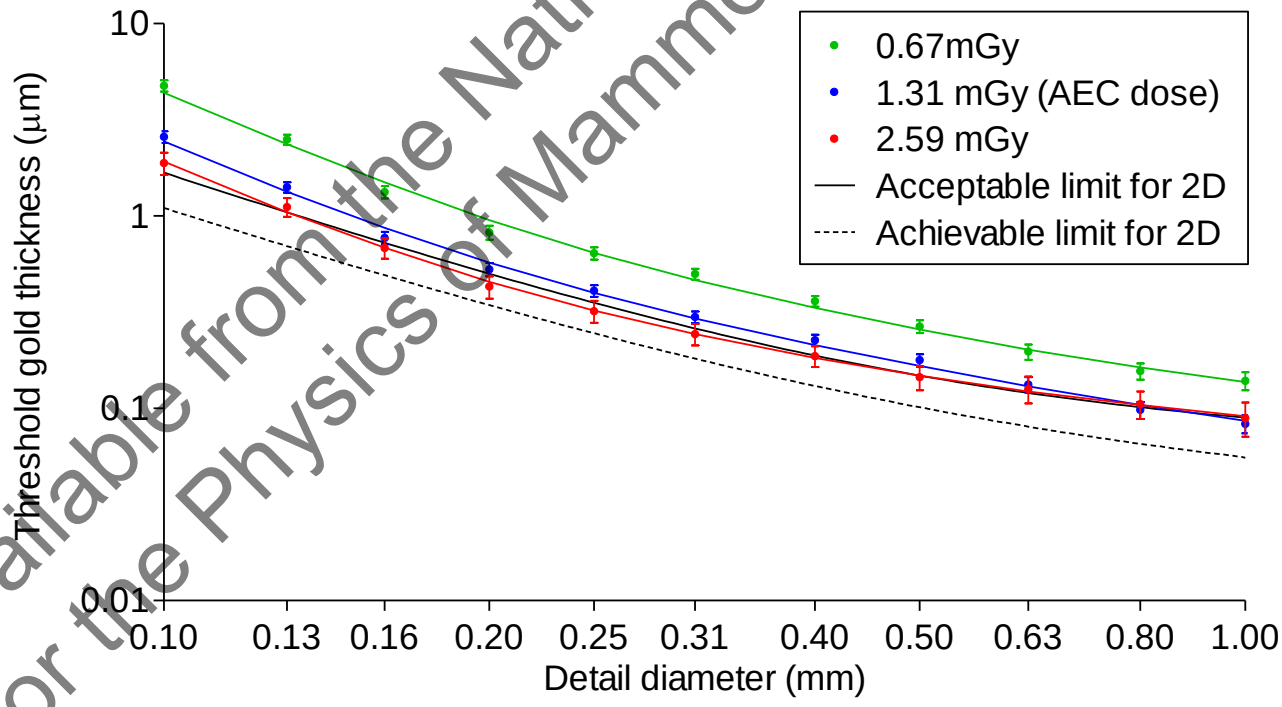

Figure 11. Threshold gold thicknesses for slab 5 from reconstructed tomosynthesis images acquired at three doses at 29kV Rh / Rh. (Error bars indicate 95% confidence limits.)

Table 11. Fit to predicted threshold gold thicknesses for reconstructed focal plane number 46 and slab number 5

	Threshold gold thickness (µm)					
Detail diameter (mm)	Focal plane AEC dose 1.31mGy	Focal plane Half dose 0.67mGy	Focal plane Double dose 2.59mGy	Slab AEC dose 1.31mGy	Slab Half dose 0.67mGy	Slab Double dose 2.59mGy
0.1	1.276	2.336	0.763	2.446	4.366	1.920
0.25	0.244	0.392	0.196	0.398	0.644	0.322
0.5	0.110	0.166	0.090	0.166	0.257	0.148
1.0	0.060	0.101	0.048	0.086	0.137	0.091

3.4 Geometric distortion and resolution between focal planes

3.4.1 Height of best focus

All balls within each image were brought into focus at the same height (±0.5mm) above the table. This indicated that the focal planes are flat and parallel to the surface of the breast support table. With the test tool taped to the underside of the compression paddle, there was slightly more variation in height, but as the paddle was not in contact with the top of the PMMA stack, it is likely to have been slightly tilted.

The first 5 focal planes, which represent 2.5mm, are below the breast support table, as shown by the heights of the balls within the reconstructed images. The number of focal planes reconstructed is equal to twice the indicated breast thickness in mm plus ten. This shows that an additional five planes are also reconstructed above the base of the compression paddle.

3.4.2 Positional accuracy within focal plane

There was no significant distortion or scaling error within focal planes. Scaling errors in both the x and y directions were found to be less than 0.3%.The maximum deviation from the mean separation between the balls was 0.3mm in the x direction and 0.2mm in the y direction, while the test object's manufacturing specification was a non-cumulative positioning accuracy of ±0.1mm.

3.4.3 Appearance of the ball in adjacent focal planes

The image of a 1mm diameter aluminium ball is well defined and circular in the plane of best focus, as shown in the middle frame of the second row in Figure 12. In focal planes above and below, the image of the ball becomes longer and fainter, with a dark area to

one side. The direction of elongation is parallel to the CWE. Figure 12 shows images of one ball, in planes 2.5mm apart, from 17.5mm below to 17.5mm above the height of the ball.

In planes at increasing heights, the images of the balls shift slightly towards the centre of the CWE. This is due to magnification effects. In the plane of best focus, balls near the lateral edges of the image have slight dark shadows on the side nearest the midline.

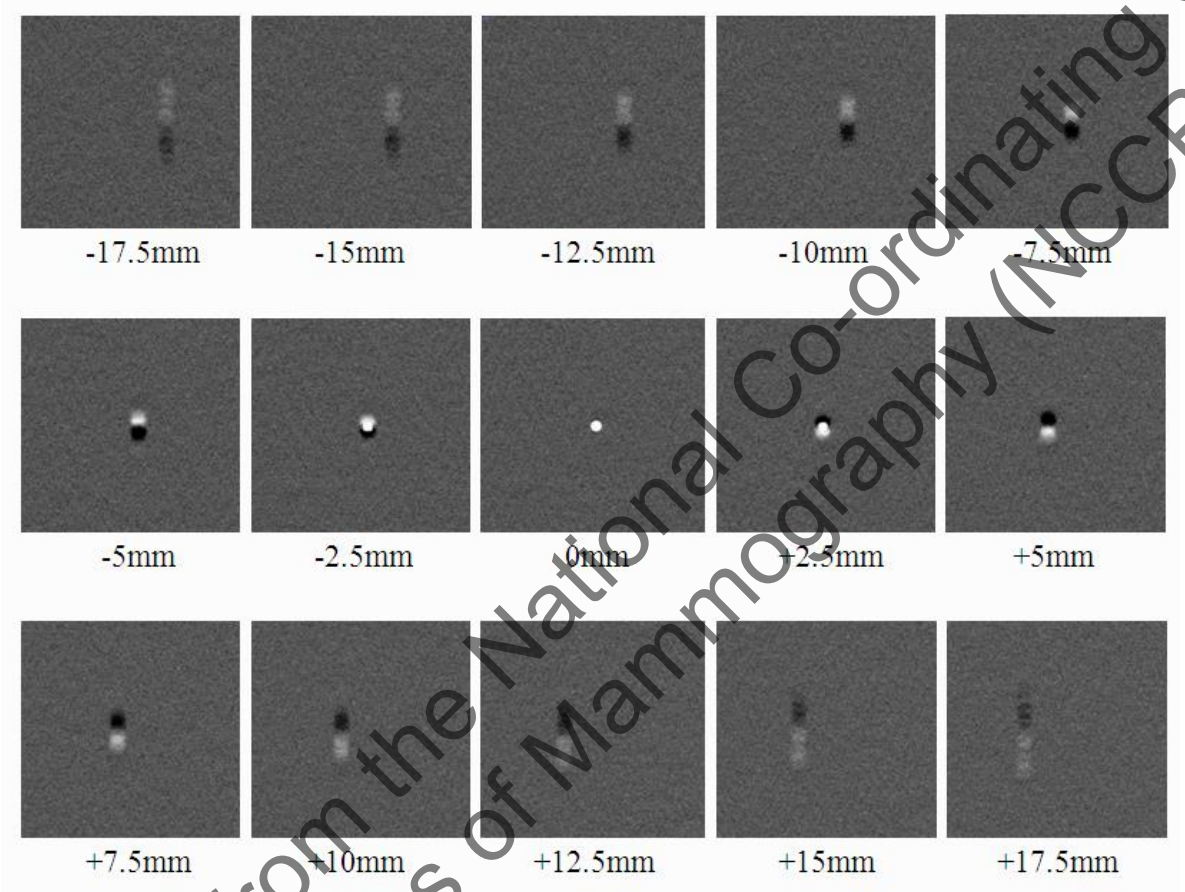

Figure 12. Appearance in focal planes at different heights of a 1mm aluminium ball, 110mm from the CWE, in the central area of a tomosynthesis image

Using DICOM viewer software, the stack of focal planes can be treated as though it were a true three-dimensional volume, and re-sliced vertically to produce planes in the x-z and y-z orientations. This is helpful in visualising the interplane artefact spread and is shown in Figure 13.

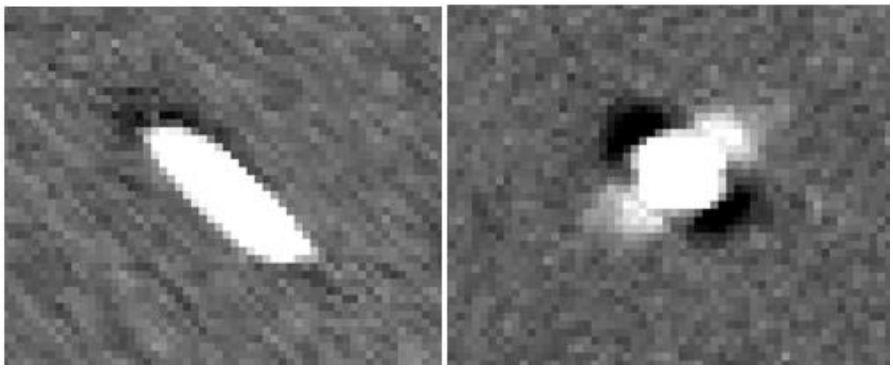

Figure 13. Vertically re-sliced planes through the centre of a 1mm aluminium ball, 110mm from the CWE, in the central area of a tomosynthesis image. (x-z plane on the left, y-z plane on the right)

Table 12 shows the results of the automated analysis of the images of balls at heights of 7.5, 32.5 and 52.5mm above the breast support table. The mean and range of x- and y-FWHM from the plane of best focus, and the composite FWHM (from all planes) are shown. The difference between these quantities indicates the apparent shift or spread of the image between planes.

Table 12. Mean values of FWHM for 1mm diameter aluminium balls and their associated reconstruction artefacts, with ranges in brackets

	FWHM within plane of best focus (mm)	Composite FWHM using all planes (mm)	Apparent shift or spread between focal planes (mm)
x (perpendicular to CWE)	0.86	1.30	0.45
	(0.80 to 0.90)	(0.83 to 1.97)	(0.00 to 1.06)
y (parallel to CWE)	0.84	1.14	0.29
	(0.80 to 0.87)	(0.84 to 1.44)	(0.00 to 0.61)
z (vertical)		6.0	
		(5.6 to 6.5)	

The variation of FWHM measurements with position within the reconstructed image are presented graphically in Figures 14 to 16.

Figure 14 shows that the composite x-FWHM (perpendicular to the CWE) increases with distance from the CWE of the image. The composite y-FWHM (parallel to the CWE) increases with distance from the middle of the CWE as shown in Figure 15.

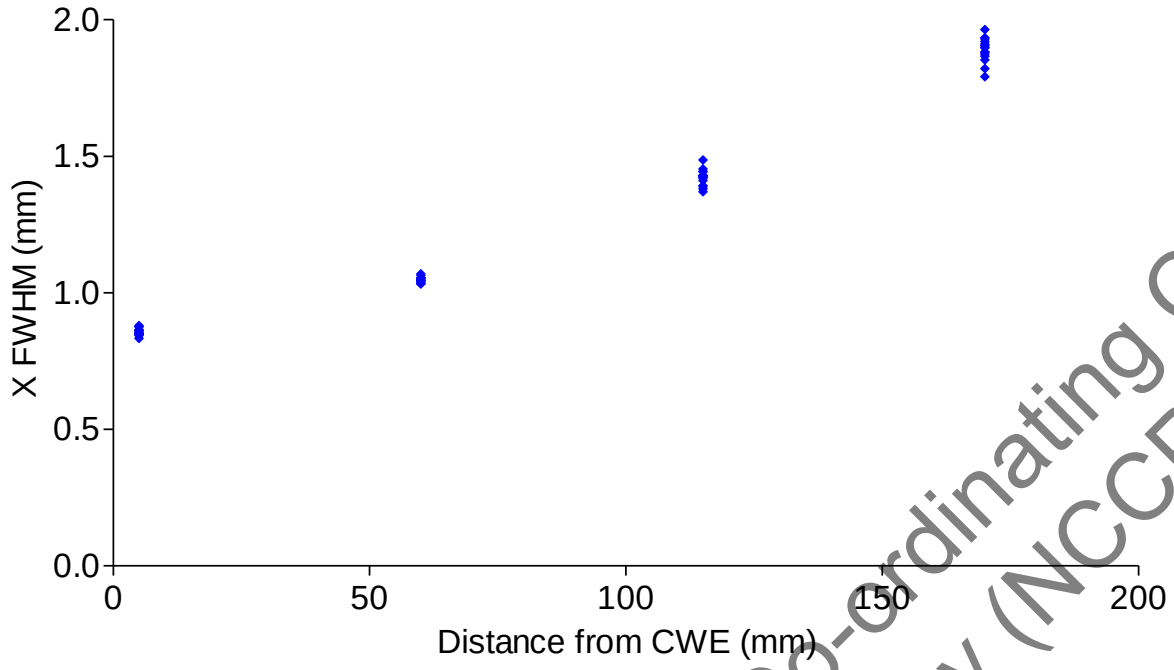

Figure 14. Composite FWHM in the x direction (perpendicular to the CWE) plotted against distance from the CWE

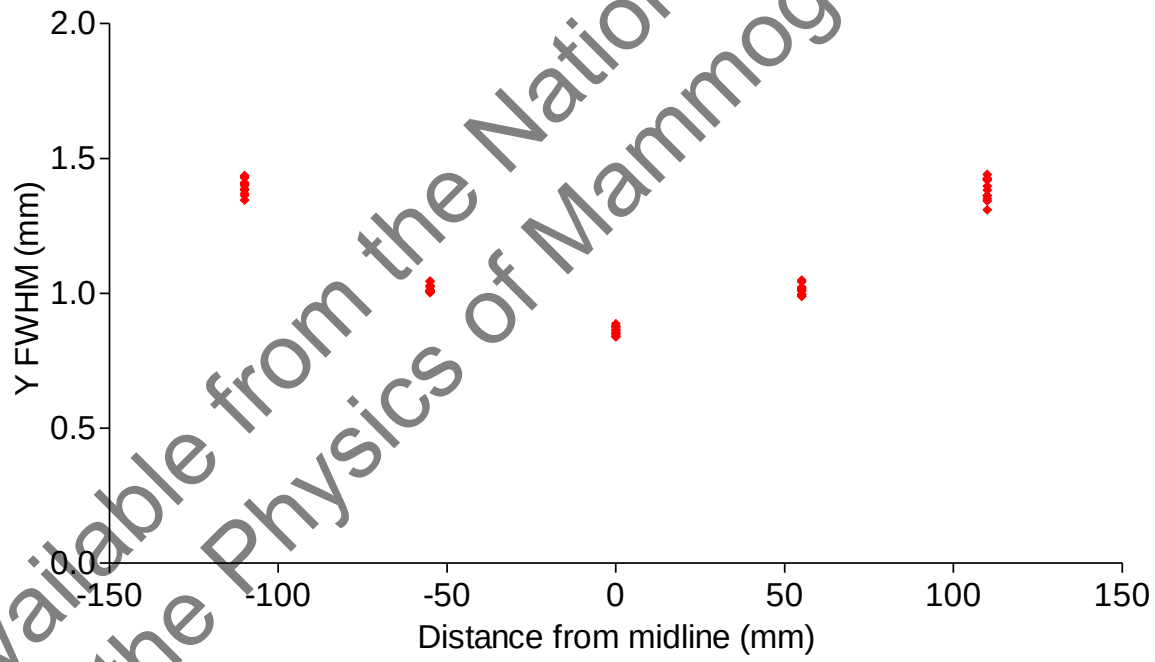

Figure 15. Composite FWHM in the y direction (parallel to the CWE) plotted against distance from the middle of the CWE

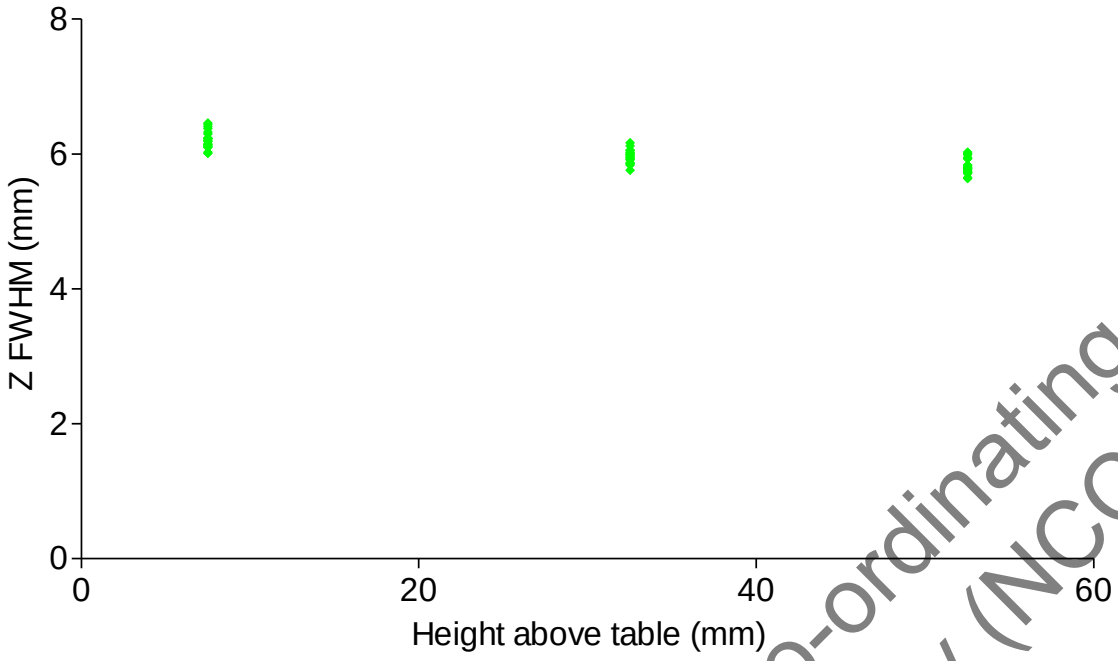

Figure 16. Composite FWHM in the z direction (vertical) plotted against height above the breast support table

The composite z-FWHM measurements give a measure of the inter-plane or z-resolution for the tomosynthesis image. Figure 16 shows no significant dependence of z-FHWM on position within the image. This was surprising because the balls nearer to the side edges appear to persist through a greater number of adjacent focal planes than balls in the central part of the image.

On further investigations of the composite z-FWHM measurements, it was found that the shape of vertical signal profiles for images of balls changes with position in the image. Figure 17 shows how the balls on the left side of the image persist through more focal planes than those on the right side. The whole focal plane within which the aluminium balls (with the CWE on the left) are brought in focus, is shown on the left of the figure. On the right of the figure, strips of images for the rectangle marked in yellow are shown for focal planes at heights of 7, 14 and 21mm above the plane of best focus, with the balls labelled from A to E.

In other images balls on both sides of the image persisted further than balls in the central area of the image. Figure 18 shows vertical signal profiles through balls A to E. These profiles show that the five balls have the same FWHM but different shapes. Measurements across the width of the vertical profile at less than the half maximum would have demonstrated the variation seen.

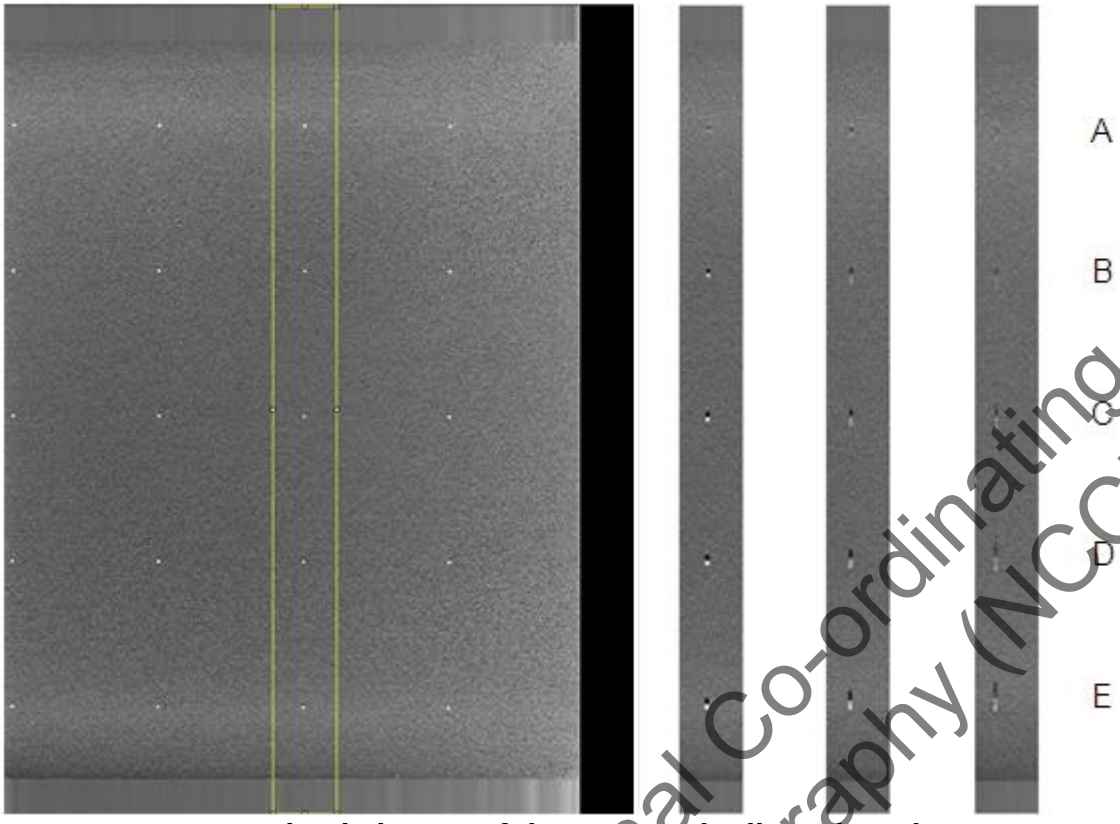

Figure 17. Tomosynthesis image of the geometric distortion phantom

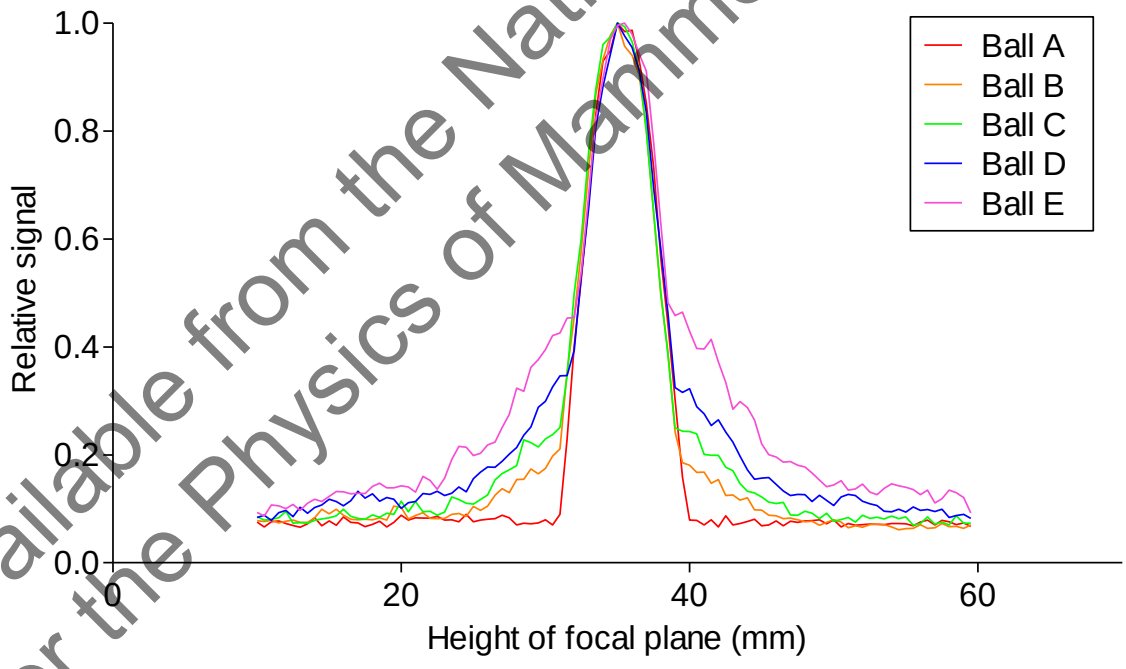

Figure 18. Vertical signal profiles though the five balls within the yellow rectangle shown in Figure 17

3.5 Alignment

At the CWE the X-ray field overlapped the reconstructed tomosynthesis image by up to 6mm at the height of the surface of the breast support table. It was difficult to locate the lateral edges of X-ray beam exactly on the self-developing film, particularly for the 18x24 field size, but the edges of the beam were seen. They were estimated to overlap the edges of the reconstructed image by up to 8mm, thus remaining well within the boundaries of the breast support table.

Small high contrast objects positioned on the breast support table were in focus in focal planes 1 to 2mm from the bottom of the reconstructed volume. Those attached to the underside of the compression paddle (when no compression was applied) were in focus in planes approximately 3 to 5mm from the top. With 9kg compression applied and the CWE of the paddle supported, the object at the top of the volume at the centre of the CWE was brought into focus in the top focal plane. Missed tissue at the CWE was not assessed.

3.6 Image uniformity and repeatability

The AEC selected the same tube voltage and target filter combination for all sixteen plain PMMA images. It used the same tube load of 55mAs for fifteen of them and 65mAs for the remaining one. This is equivalent to a maximum deviation of 17% from the mean dose.

The maximum deviation from the mean SNR measured in the sixteen images of plain PMMA was 1.6%.

Large format (24cm x 30cm) reconstructed focal planes were obscured along the left and right edges of each focal plane by a grey band which contained no useful information. The width of the bands varied with height, from approximately 6mm at the table surface to 14mm at a height of 50mm above the table. This band can be seen in the geometric distortion image shown in Figure 17.

Apart from increased pixel values towards the lateral edges, the reconstructed focal planes appeared to be generally fairly uniform, with the following subtle artefacts visible:

1. In reconstructed images of plain PMMA, faint parallel lines running perpendicular to the CWE were sometimes seen covering parts of the focal plane. This effect was not noticeable on images containing detail, such as CDMAM images.

2. A row of a few white spots (with raised pixel value), of approximately 1mm diameter, were sometimes seen along the lateral edge of a focal plane, at the very edge of the reconstruction.

3.7 Detector response

The detector response, measured using the MTD in tomosynthesis and 2D modes, is shown in Figure 19. The anti-scatter grid remained in position for these measurements. No grid transmission factor correction was applied for the entrance air kerma per image or projection.

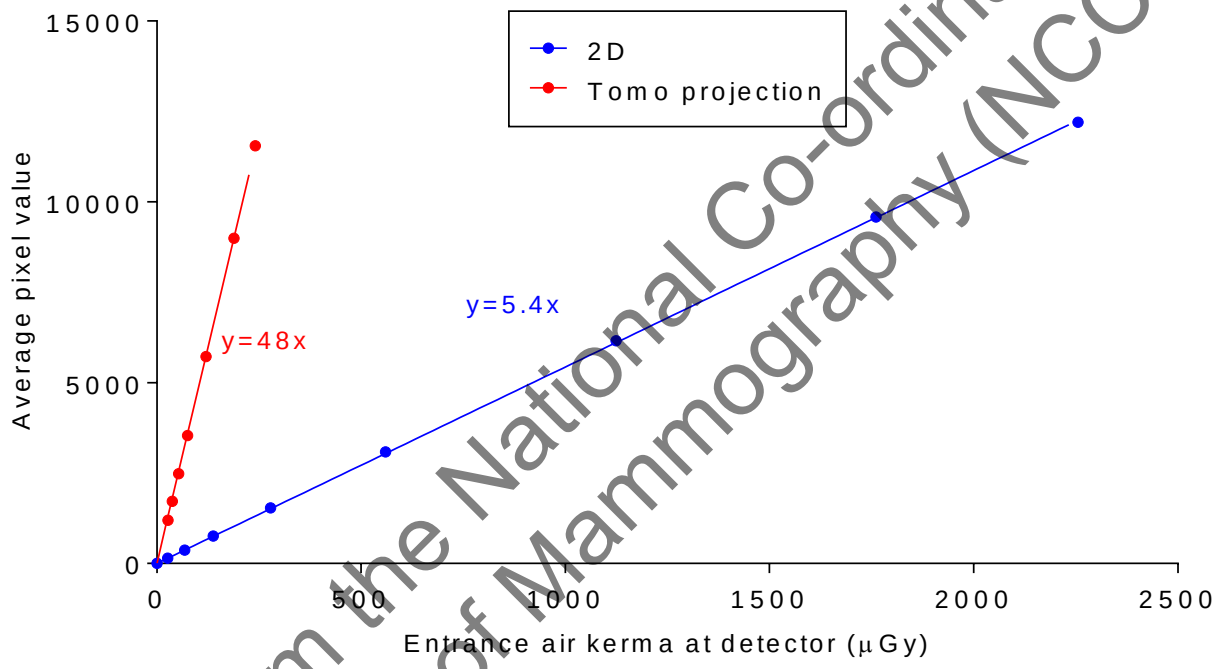

Figure 19. Detector response (anti-scatter grid included) using the MTD, for 2D and tomosynthesis modes

4. Discussion

4.1 Dose and CNR

MGDs were calculated for a range of equivalent breast thicknesses from 21mm to 117mm, exposed under AEC. The MGDs were well within the NHSBSP dose limits for 2D mammography for both of the 2D modes (2D Bucky and MTD, in Standard mode)

and for the tomosynthesis mode. MGDs for 2D exposures made with the MTD were 1-30% higher (on average 15% higher) than those made with the 2D Bucky. MGDs for tomosynthesis exposures were similar to those for 2D exposures made with the MTD. For a 53mm equivalent breast thickness, the MGDs were 1.13mGy, 1.29mGy and 1.09mGy for exposures made with the 2D Bucky, the MTD in 2D mode and in tomosynthesis mode, respectively. The NHSBSP dose limit for 2D mammography is 2.5mGy for this thickness.

In 2D mode, when using either the 2D Bucky or the MTD under AEC (Standard mode), the CNRs for all equivalent breast thicknesses exceeded the value required to meet the NHSBSP standard for minimum acceptable image quality. For equivalent breast thicknesses up to 60mm, the CNRs exceeded the value for achievable image quality. As expected, the CNRs decreased significantly as thickness increased, so it might be advisable to increase the dose for larger breasts, by using Contrast mode for example.

The estimated doses to reach the target CNRs for the minimum acceptable and achievable levels of image quality were 0.52 ± 0.10mGy and 1.13 ± 0.23mGy respectively when using the 2D Bucky. They were 0.58 ± 0.12mGy and 1.26 ± 0.25mGy respectively for 2D imaging using the MTD. These results for the 2D Bucky are close to the values previously reported for the GE Healthcare Essential: 0.49 ± 0.10mGy and 1.13 ± 0.23mGy.

CNR values in reconstructed tomosynthesis focal planes are expected to be highly dependent on the degree of smoothing and scaling inherent within the reconstruction algorithm. Any interpretation of CNR values in relation to image quality in tomosynthesis should therefore be treated with caution. The focal plane CNR and slab CNR were found to remain fairly constant across the range of breast thicknesses.

CNRs measured in the unprocessed tomosynthesis projection images also decreased with increasing thickness. The CNRs are lower than for 2D images because the dose per projection is a fraction (in this case one ninth) of the total dose.

The variation of CNR with dose in tomosynthesis images was assessed. A power fit applied to the relationship between CNR and dose for projections had an index close to 0.5. This indicates that quantum noise is the dominant noise source in the projection images. CNRs measured in reconstructed focal planes and slabs also increased with dose.

4.2 Image quality

Image quality in 2D mode was assessed for both the 2D Bucky and the MTD, using the CDMAM test object. In both cases, at a dose equal to that obtained under AEC, the 2D

threshold gold thickness curve was close to the achievable level of image quality for all detail sizes.

CDMAM images were also acquired in tomosynthesis mode, at the same dose as under AEC. The threshold gold thickness curve for reconstructed focal planes was close to the achievable level of image quality that is defined for 2D mammography for all except the 0.1mm detail. The 0.1mm value was slightly greater than the minimum acceptable standard for 2D. However, this result takes no account of the ability of tomosynthesis to remove the obscuring effects of overlying tissue in a clinical image. The degree of this effect is expected to vary in different tomosynthesis systems. At double and half the AEC selected dose, the threshold gold thickness decreased and increased, respectively, as expected. For reconstructed slabs the threshold gold thickness curve was considerably poorer than that for the focal planes, falling below the 2D minimum standard for all but the largest 1mm detail. This result suggests that the slabs should only be regarded as supplementary to the reconstructed focal planes, and should not be relied upon in isolation.

There is no standard test object available yet that would allow a realistic and quantitative comparison of tomosynthesis image quality between systems, or between 2D and tomosynthesis modes. A suitable test object would incorporate simulated breast tissue to show the benefit of removing overlying breast structure in tomosynthesis imaging, as compared to 2D imaging. In the absence of such a test object, an extensive clinical trial would be needed to determine whether the performance of a particular tomosynthesis system is clinically adequate.

4.3 Geometric distortion and reconstruction artefacts

Assessment of geometric test phantom images demonstrated that the reconstructed tomosynthesis focal planes are flat and parallel to the surface of the breast support table with no vertical distortion. The geometric distortion within the focal plane was negligible, as shown by comparing measured and true distances between imaged details. The scaling error, calculated using the pixel spacing quoted in the image DICOM headers, was also negligible.

The reconstructed tomosynthesis volume includes an additional 2.5mm below the surface of the breast support table and 2.5mm above the nominal height of the compression paddle. This allows for a small margin of error in the calibration of the indicated thickness or some slight tilt of the paddle, without missing tissue at the bottom or top of the reconstructed image.

In tomosynthesis images of 1mm diameter aluminium balls, the balls appeared circular within the plane of best focus. When viewing successive focal planes, moving away

from the plane of best focus, the balls appeared to stretch slightly then fade and separate into two broad lines, one light and one dark. These elongated in the direction parallel to the CWE, and shifted away from the centre of the CWE. This apparent shift of the reconstruction artefacts is due to the geometry of the diverging X-ray beam. The magnification effect was quantified by measuring the maximum extent of the 50% contour level in background corrected pixel values around each ball in all planes. It was greater than that in the plane of best focus by up to 1.1mm.

The 50% contour extended vertically between focal planes, giving a mean inter-plane resolution (z-FWHM) of 6mm for the 1mm diameter balls. Balls of greater or lesser diameter would result in more or less extensive reconstruction artefacts, so the inter-plane resolution would vary accordingly. Inter-plane resolution varied by less than 10% with position in the reconstructed volume.

Balls near the lateral edges of images appeared to persist through a greater number of adjacent focal planes than balls at the centre of the image. As this variation across the image was not evident in the z-FWHM measurements, this was investigated further. It was found that the shape of vertical line profiles through images of balls changed significantly with position in the image. However, the significance of this observation is doubtful, as the contrast of the aluminium balls is abnormally high compared to the contrasts expected in clinical images.

4.4 Alignment

There was no missed tissue at the top or bottom of reconstructed tomosynthesis images. Missed tissue at the CWE was not assessed.

The alignment of the X-ray beam to the reconstructed image was assessed. At the CWE the overlap was up to 6mm, compared to the limit of 5mm for 2D imaging, though the limit was only exceeded with the rarely used molybdenum target. At the other sides of the image, the edges of the X-ray beam were not sharply defined but were detected and found to overlap the edges of the image by up to 8mm, remaining well within the boundaries of the breast support table.

4.5 Image uniformity and repeatability

Faint artefacts were seen in reconstructed tomosynthesis images. These included patches of parallel lines in images of plain PMMA, and some white spots appearing in a row along the lateral edges of the reconstruction. Clinical images should be checked to ensure that such artefacts do not impinge on the clinical images. The width of large format reconstructed focal planes was restricted by grey bands up to 15mm wide along the lateral edges. These contained no information.

Repeat tomosynthesis imaging of the same phantom under AEC resulted in the same dose for fifteen images and an 18% higher dose for one, when the tube load increased by 10mAs. This suggests the existence of steps in the determination of the tube load settings for projections.

4.6 Detector response

Measurements of detector response in 2D and tomosynthesis modes showed that the amplification of the detector signal is greater in tomosynthesis mode than in 2D mode.

5. Conclusions

The technical performance was tested in both 2D and tomosynthesis modes. Doses for 2D images were on average 15% higher for the MTD compared to the standard 2D Bucky. 2D imaging performance, using either the 2D Bucky or the MTD, met current NHSBSP standards for digital mammography, with no significant difference in image quality.

The MGDs measured in tomosynthesis mode were found to be close to those measured in 2D mode when using the MTD. The tomosynthesis doses are well within the NHSBSP dose limits for 2D mammography.

No performance standards have yet been set for digital breast tomosynthesis systems, and it is not yet possible to predict clinical tomosynthesis performance from these results.

References

1. Workman A, Castellano I, Kulama E et al. *Commissioning and Routine Testing of Full Field Digital Mammography Systems* (NHSBSP Equipment Report 0604 Version 3). Sheffield: NHS Cancer Screening Programmes, 2009

2. van Engen R, Young KC, Bosmans H et al. The European protocol for the quality control of the physical and technical aspects of mammography screening. In: *European Guidelines for Quality Assurance in Breast Cancer Screening and Diagnosis*, 4th Edition. Luxembourg: European Commission, 2006

3. van Engen R, Bosmans H, Dance D et al. Digital mammography update: European protocol for the quality control of the physical and technical aspects of mammography screening. In: *European guidelines for quality assurance in breast cancer screening and diagnosis,* Fourth edition – Supplements. Luxembourg: European Commission, 2013

4. Strudley CJ, Looney P, Young KC. *Technical evaluation of Hologic Selenia Dimensions digital breast tomosynthesis system* (NHSBSP Equipment Report 1307 Version 2). Sheffield: NHS Cancer Screening Programmes, 2014

5. Strudley CJ, Warren LM, Young KC. *Technical evaluation of Siemens Mammomat Inspiration digital breast tomosynthesis system* (NHSBSP Equipment Report 1306 Version 2). Sheffield: NHS Cancer Screening Programmes, 2015

6. Strudley CJ, Young KC, Oduko JM et al. Development of a Quality Control Protocol for Digital Breast Tomosynthesis Systems in the TOMMY Trial. In: *International Workshop on Breast Imaging 2012.* Berlin: Springer-Verlag, 2012, 330–337

7. Young KC, Oduko JM, Gundogdu O, Alsager A. *Technical Evaluation of the GE Essential Full Field Digital Mammography System* (NHSBSP Equipment Report 0803). Sheffield: NHS Cancer Screening Programmes, 2008

8. Young KC, Oduko JM, Gundogdu O, Asad M. *Technical Evaluation of Profile Automatic Exposure Control Software on GE Essential Full Field Digital Mammography Systems* (NHSBSP Equipment Report 0903). Sheffield: NHS Cancer Screening Programmes, 2009

9. *Digital Imaging and Communications in Medicine (DICOM) Part 3: Information Object Definitions.* Virginia: National Electrical Manufacturers Association, 2011

10. Dance DR, Young KC, van Engen RE. Estimation of mean glandular dose for breast tomosynthesis: factors for use with the UK, European and IAEA breast dosimetry protocols. *Physics in Medicine and Biology,* 2011, 56: 453-471

11. Dance DR and Young KC, 2014, private communication

12. Boone JM, Fewell TR and Jennings RJ. Molybdenum, rhodium and tungsten anode spectral models using interpolating polynomials with application to mammography *Medical Physics,* 1997, 24: 1863-1974

13. Berger MJ, Hubbell JH, Seltzer SM Chang et al. XCOM: Photon Cross Section Database (version 1.3) http://physics.nist.gov/xcom (Gaithersburg, MD, National Institute of Standards and Technology), 2005

Appendix 1: Manufacturer's comment

The manufacturer has added the following comment which is not part of the current evaluation

- with reference to the synthetic 2D view (Section 2.1), since this evaluation was performed, it has been made available for download as a BTO object